THICK LIQUID-WALLED, FIELD-REVERSED CONFIGURATION*

R. W. Moir[a], R. H. Bulmer[a], K. Gulec[b], P. Fogarty[c], B. Nelson[c], M. Ohnishi[d], M. Rensink[a], T. D. Rognlien[a], J. F. Santarius[e], and D. K. Sze[f]
[a]Lawrence Livermore National Laboratory, P. O. Box 808, L-637,
Livermore, CA 94550, Tel: 925-422-9808
[b]43-133 Engineering IV, Box 951597University of California, Los Angeles, CA 90024
[c]Oak Ridge National Laboratory, Oak Ridge, TN 37831-8218
[d]Kansai Univ, 3-35, Yamate-cho 3 chome, Suita-shi, Osaka, Japan
[e]University of Wisconsin, 1500 Engineering Dr. Madison, Wisc 53706
[f]Argonne National Laboratory, 9700 South Cass Ave, Bldg 207, Argonne, IL 60439

Abstract
A thick flowing layer of liquid (e.g., flibe—a molten salt, or $Sn_{80}Li_{20}$—a liquid metal) protects the structural walls of the field-reversed configuration (FRC) so that they can last the life of the plant even with intense 14 MeV neutron bombardment from the D-T fusion reaction. The surface temperature of the liquid rises as it passes from the inlet nozzles to the exit or receiver nozzles due to absorption of line and bremsstrahlung radiation, and neutrons. The surface temperature can be reduced by enhancement of convection near the surface to transport hot surface liquid into the cooler interior. This surface temperature must be compatible with a practical heat transport and energy recovery system. The evaporative flux from the wall driven by the surface temperature must also result in an acceptable impurity level in the core plasma. The shielding of the core by the edge plasma is modeled with a 2D transport code for the resulting impurity ions; these ions are either swept out to the distant end tanks, or diffuse to the hot plasma core. An auxiliary plasma between the edge plasma and the liquid wall can further attenuate evaporating flux of atoms and molecules by ionization. The current in this auxiliary plasma might serve as the antenna for the current drive method, which produces a rotating magnetic field. Another method of current drive uses small spheromaks injected along the magnetic fields, which additionally provide fueling along with pellet fueling if necessary.

1. Introduction

This paper discusses the present understanding of a future power plant based on a field-reversed configuration (FRC) with a liquid first wall. Although expected to be unstable to ideal MHD modes, experimental FRC plasmas have proved to be relatively stable and robust. This may be due to the finite ratio of plasma radius to average gyroradius (called s; see Table 1) in present experiments, which is one of several non-ideal MHD considerations that remain difficult to treat theoretically. In a fusion power plant, for example, the large gyroradii of the fusion products are also expected to contribute to stability. An FRC fusion core would have to be designed to be macroscopically stable, because unstable plasmas would give excessive plasma energy losses. The main focus of this paper is on liquid wall features rather than plasma stability, however, so this and other important unanswered questions, such as plasma transport due to microinstabilities, will not be treated here. Research teams at the University of Washington[1] and elsewhere are experimentally trying to achieve a working model using rotating magnetic fields to build up and sustain the FRC and see if the predicted high loss rates will nevertheless allow a practical power plant. The predicted power density is so high with the DT reaction that liquid walls are almost a necessity. Alternatives are to use the D^3He cycle as discussed in Ref. 2 or change out damaged first walls and structures often. The Astron power plant concept[3] was an early FRC that proposed using liquid walls.

This study is part of the (Advanced Power EXtraction) APEX[4] project, which is investigating innovative blanket concepts, with liquid wall systems as a major option and is a work in progress. The underlying logic is to provide up to about 7 mean free paths of liquid for 14 MeV neutrons between the plasma and structures including the first wall so that these structures last the life of the plant. The structures satisfy the rough criterion that the damage should be less than 100 dpa (displacements per atom) and still fall within design specifications. It would be useful to develop a damage criterion versus liquid thickness for materials such as flow baffles that perform a reduced function (i.e., nonstructural function). This liquid is injected as shown in Fig. 1 by nozzles that give the liquid enough azimuthal speed that centrifugal force keeps it against the wall even when the orientation as shown is horizontal. Vertical orientation might have advantages and be necessary with liquid metals. The flow is very nearly along field lines so that even liquid metals such as lithium or tin-lithium mixtures could work, however our main example is to see if the molten salt called flibe[5] (a mixture of LiF and BeF_2) will be workable. One of the virtues of flibe is its compatibility with stainless steel such as 304SS,

if the chemistry associated with transmutation products can be controlled.

A set of FRC parameters is given in Table 1. These parameters are not all self-consistent with cases treated throughout the paper. Studies based on the tokamak configuration show the evaporation of the flibe principally BeF_2 molecules will overwhelm the burning plasma (put it out), however, the FRC may be different in that the edge plasma should not easily return from the wall in the end tanks (low recycle mode). This leads us to consider adding auxiliary edge plasma feed by a "gas box" from each end through an annular slot. The configuration is shown in Fig.2.

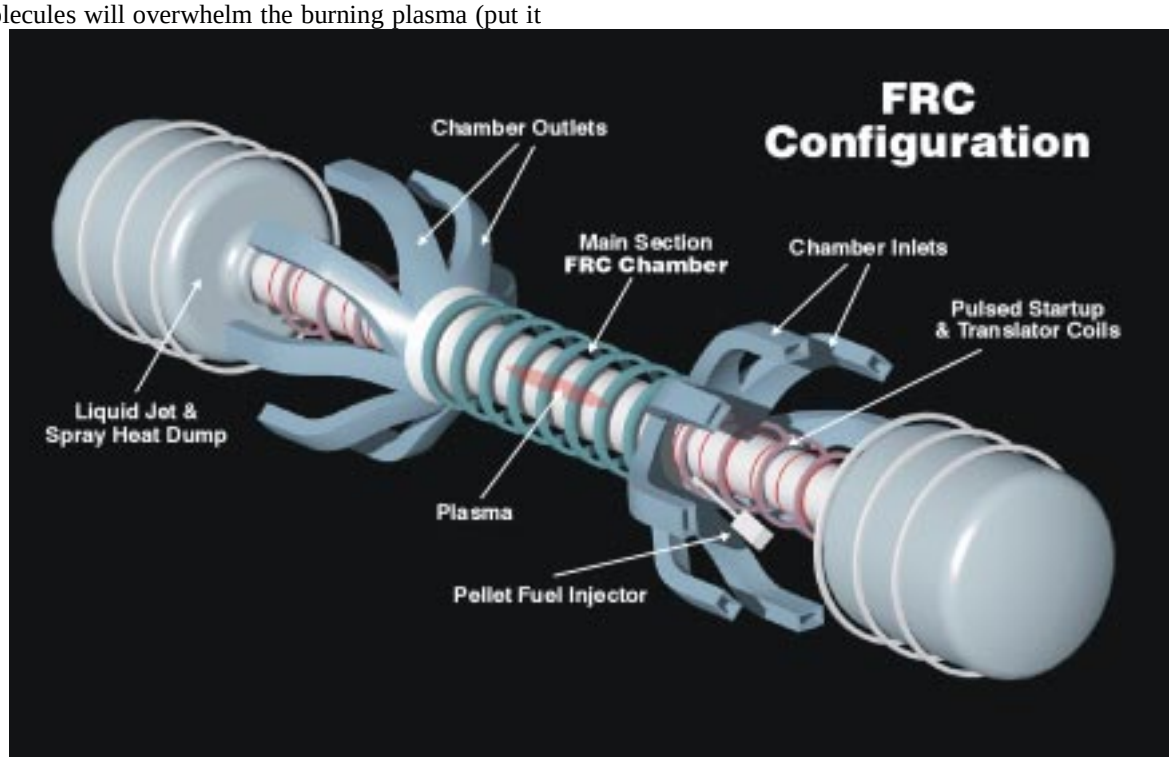

Figure 1**.** General layout of a FRC power plant design.

2. Hydraulics and the inlet and outlet nozzles

Hydraulics studies using 3D computational fluid dynamics codes show the feasibility of providing the flow pattern called for in Fig. 3. There is the question of nozzle design. The nozzles are exposed to neutrons so that their damage-limited lifetime needs to be determined. The inlet nozzle must not have excessive dripping that might cause core plasma contamination. Device orientation is important as vertical orientation, shown later in Fig. 8, could allow drips to miss the plasma in their vertical fall. The exit or receiver nozzles appear to be much more difficult. Splashing and choking will need to be strictly avoided. If the cross-sectional area of the exit nozzle is larger than that of the flowing liquid then choking might not occur. Once the flowing liquid is contained within the exit channel, it can be directed outside the chamber and then voids can be eliminated and the flow can be slowed down in a diffuser where its kinetic energy can be converted into potential energy (pressure=$0.5\rho v^2$). Vertical orientation will help in design of the exit nozzles and the diffuser. The acceleration-thinning problem in vertical orientation can be partially compensated by inserting flow baffles with the possible addition of azimuthal flow to prevent the flow over the baffles from entering the core plasma region. Another solution is just to start with a thicker layer.

3. Mass flow and temperature diagram

We assume a 50-degree drop across the heat exchanger. This is a compromise, as we would like 100 degrees. The HYLIFE-II heat transport system[6] assumes 100 degrees drop across the heat exchangers, which are also the steam generators. The cost estimate for the heat transport system is 174 M$ out of a total direct cost of 1440 M$ for a 1 GWe plant and 338 M$ out of 2240 M$ for 2 GWe (1995$). If we assume a 50-degree drop will increase these costs by $2^{0.7}$ then the plant costs will increase by 7.5 and 9.5% for the 1 and 2 GWe plants, respectively. This is a large cost increase, which will have to be studied more to see if our choice is prudent. Our driving motivation is to reduce the surface temperature to limit the evaporative flux, which is directed toward the core plasma. We assume the molten salt from the heat exchanger is mixed with the bypass flow to a mixed mean temperature, 540 °C, which is then fed to the inlet nozzles. It might be possible to feed the 500 °C cooler molten salt from the heat exchanger

Table 1: Typical D-T FRC Power Plant Parameters.

	Liquid-Wall FRC	Solid-Wall FRC	D^3He (ref. 2)
Wall radius, m	1.5	2.0	2.0
Separatrix radius, m	0.39	0.88	1.1
Separatrix length, m	8	25	17
Core plasma volume, m^3	2.6	26	67
First-wall area, m^2	75	314	215
Average ion temperature, keV	12	13	88
Average ion density, 10^{20} m^{-3}	26	8.3	6.6, n_e
Peak ion density, 10^{20} m^{-3}	31	8.6	
Zeff	1.5	1.5	
s = plasma radius/ average larmor radius	7.5	4.3	9.2
Volume-averaged beta	0.97	0.90	0.9
Magnetic field, T	5.5	3.0	6.7
Energy confinement time, s	0.08	0.31	2.1
Ash particle conf. time, s	0.16	0.62	4.2
Neutron wall load, MW/m^2	27	6.4	0.4
Surface heat load, MW/m^2	1.7	0.236	1.7
Neutron power, MW	2000	2000	80
Bremsstrahlung radiation power, MW	46	44	360
Line radiation @ 15% P_{alpha}, MW	78	70	
Charged-particle transport power, MW	415	426	1160
Input power, MW	40	40	
Fusion power, MW	2500	2500	1600
Net electric power, MWe	1000	1000	1050

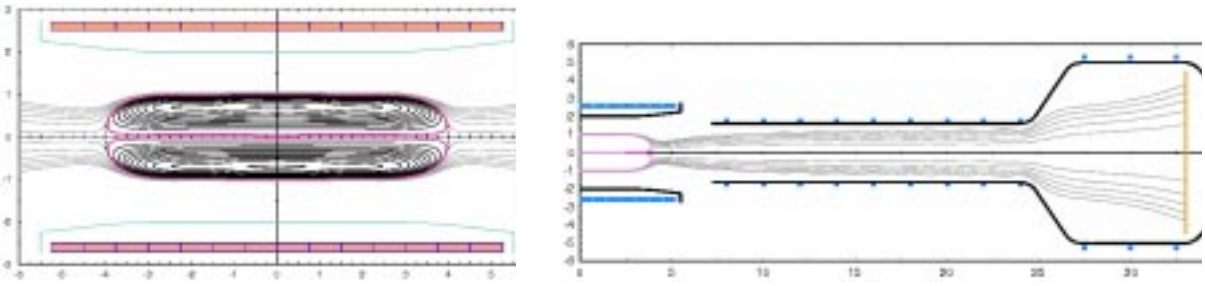

(a) (b)

Figure 2. FRC configuration. The MHD equilibrium calculation using Corsica is shown in (a) and the edge plasma leading out to the end tanks is shown in (b).

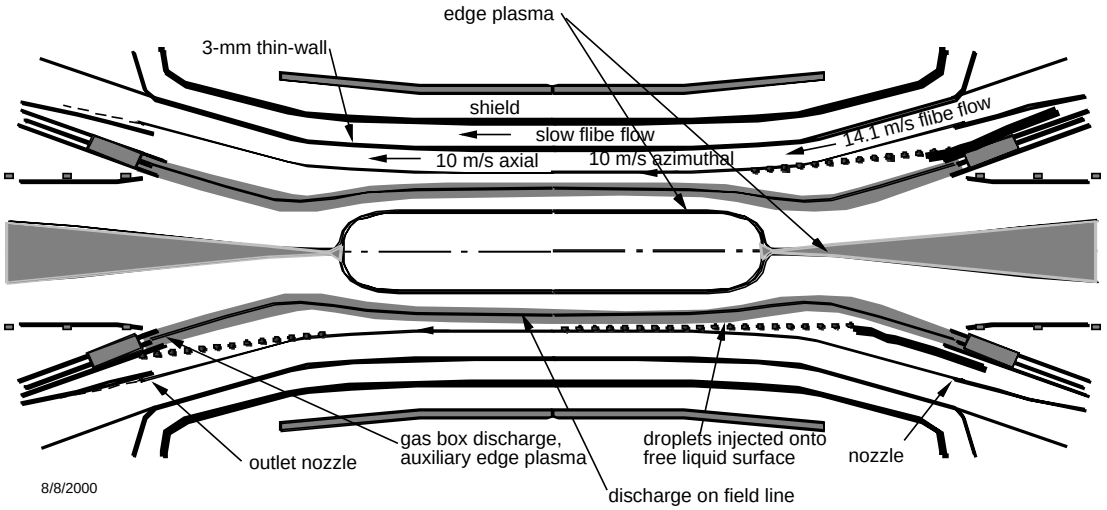

Figure 3. FRC showing the liquid flow, antenna current drive, gas box and pellet injector.

directly to the nozzles feeding the surface flow. We assume a heat exchanger outlet temperature of 500 °C. This leaves 40 °C above the freezing temperature. In the future the melting point could be lowered by about 30 degrees by reformulating the salt mixture. This would lower the salt temperature facing the plasma.

In order to arrive at 1000 MWe we assume a 2400 MW fusion power with blanket multiplication of 1.18. The blanket power is 2400 ×(0.8×1.18+0.2) = 2750 MW. The volumetric flow rate and mass flow rates are:
$V' = \pi(2^2-1.5^2)$ 10 m/s = 55.0 m^3/s

$m' = V' \times 2000$ kg/m^3 = 1.10×10^5 kg/s

The temperature rise on average passing through the blanket and shield is:
$\Delta T = P/m'C = 2.75\times10^9$ J/s/(1.10×10^5 kg/s 2380 J/kgK) = 10.5 °C
The mass flow rate to the heat exchanger is:
$m'=2.7456\times10^9$ J/s/(50°C × 2380 J/kgK) = 2.31×10^4 kg/s
If we take an axial flow speed of 10 m/s and a nominal 10 m/s azimuthal flow then the power in the flowing liquid, which is a measure of the pumping power with no head recovery, is as follows:
Power = $0.5m'v^2$ = $0.5 \times1.1\times10^5$ kg/s × (10^2 + 10^2) m^2/s^2 = 1.1×10^7 W = 11 MW. The above parameters are shown in the mass flow diagram, Fig. 4. For the case of SnLi with the same thickness as flibe and 10 m/s flow along the field lines, we get a pumping power of 16.5 MW and assuming 100 °C across the heat exchangers we get the temperatures shown in parentheses in Fig. 4. The flow that bypasses the heat exchanger is 3.8 times that through the heat exchanger. It would be desirable to have all of the heat exchanger flow go to the blanket but then the flow speed rather than being 10 m/s would only be 2.7 m/s and the temperature rise discussed next would be very large resulting in high evaporation rates.

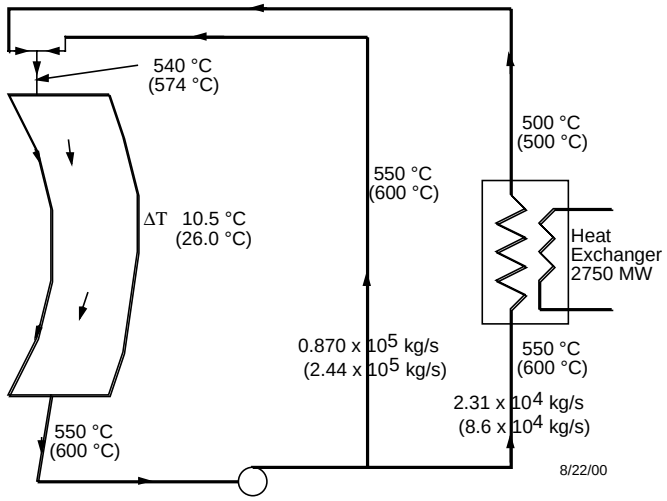

Fig. 4. Mass flow and temperature diagram for the FRC. The numbers shown are for flibe with the SnLi values shown in parentheses.

4. Heat transfer model and estimates of effective surface temperature

The temperature of the surface can be calculated knowing the heat load and the heat transfer characteristics of the liquid. The idea is to follow a fluid element on the surface from the time it leaves a nozzle till it enters an exit nozzle. The complications are many. The radiation can be absorbed over a distance larger (deeper) than the thermal diffusivity distance x, which is the distance in a time, t, heat diffuses ($x^2=tk/\rho c$). C is the heat capacity, ρ is the mass density and k is the thermal conductivity. As an example, x = 0.47 mm for flibe and 4.2 mm for SnLi in 1

s. The mean free path for typical Bremsstrahlung x-rays is 3 mm and 0.03 mm for flibe and SnLi, so that volumetric heating (Eq.5) is used for flibe but surface heating for SnLi (Eq. 4). In this case the surface temperature is less than if all the incident energy flux were absorbed on the surface. The other complication is the heat transfer can be greater for turbulent flow than for laminar flow. Heat conduction is a diffusive process. Reynolds analogy is the observation that mass transfer and heat transfer are analogous processes. Mass diffusion will carry heat when there is a temperature gradient just like heat is conducted (diffused). Mass transfer can be small due to molecular collisions or can be enhanced by the action of turbulent eddies. Steady heat conduction is governed by the equation:

$$P/A = k dT/dx \quad (1)$$

Where P/A is the power flux striking the surface that penetrates a distance short compared to the thermal diffusivity distance mentioned above. Guided by Reynolds analogy, we argue that this equation can be modified to account for enhanced heat transfer by eddy motion.

$$P/A=(k+k')dT/dx \quad (2)$$

$$k_{eff} = k + k' = k (1+F) \quad (3)$$

The parameter F represents the enhancement of heat conduction due to turbulence. When F = 0 the flow is laminar. When F=1 the thermal conductivity is doubled. Magnetic fields will tend to laminarize the flow reducing F. Flow baffles can be added to create eddies or jets embedded in the liquid can enhance eddy motion which propagates to the surface both of which tend to increase k_{eff}. Large values of k_{eff} might be possible with flibe where the electrical conductivity is so low that turbulence may play a large role. In the analysis to follow, F or k_{eff} is treated as a parameter because it is unknown; however, theoretical work by Smolentsev[7] and his planned experiments (e.g., flow baffles) should allow us to predicted k_{eff}.

Another idea to produce enhanced mixing (large k_{eff} values) is to spray droplets onto the surface. They must be small enough not to cause splash and large enough to cause persistent vortex motion. The idea and a relevant simulation[8] are shown in Fig. 5.

The temperature of the surface of the fluid element as we ride along as shown in Fig. 3 is then given by the equation

$$T = T_{inlet} + 2 (P/A) (t/\pi\rho c k_{eff})^{0.5} \quad (4)$$

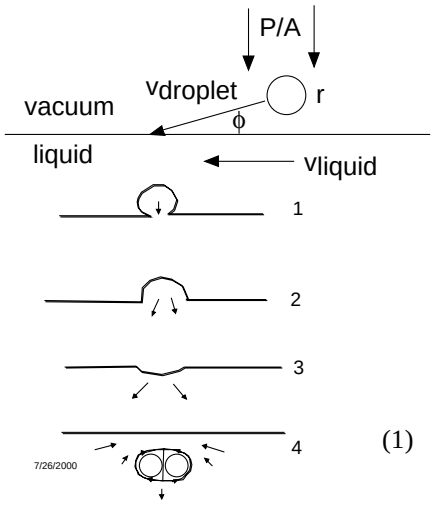

Fig. 5. The idea of droplets sprayed on a surface causing convection with no splash is shown on the left. A simulation is shown on the right with Reynolds number=$2vr/\nu$=20 and Weber number=$\rho r v^2/\sigma$=2.

A key parameter is the incident power flux, P_{wall}/A on the liquid surface. For the FRC we assume 3% of the fusion power of 2400 MW is in the form of non-penetrating radiation such as line radiation which directly heats the surface or 78 MW, which is taken to be 15% of the alpha power and may be low (20 to 40% is commonly assumed). With a surface area of 75 m^2, the P_{wall} (MW) /A (m^2) = 1.0 MW/m^2 . The temperature rise versus time is plotted in Fig. 6.

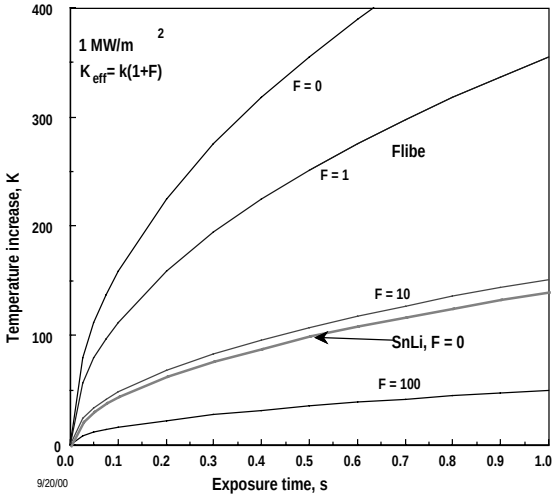

Fig. 6. Temperature rise of the fluid element versus time at 1.0 MW/m^2. F is the thermal conductivity enhancement factor to account for near surface turbulence or convection.

The temperature rise due to penetrating power flux due to neutrons and bremsstrahlung cause a temperature rise.

$$T = T_{inlet} + \frac{P}{V}\frac{\tau}{\rho c} \quad (5)$$

The temperature rise is

$$\Delta T = T_{out} - T_{inlet} = \Delta T_{neutron} + \Delta T_{line} + \Delta T_{brem} + \Delta T_{cyclotron} + \Delta T_{particlesonwall} \quad (6)$$

We include in Eq. 6 surface temperature rise due to cyclotron radiation and particle bombardment such as charge exchange neutrals, altahough we have neglected them in our calculations to date. The temperature rise in 0.8 s for flibe is 141 °C for line radiation, 34 °C for bremsstrahlung and 32°C for neutron heating and for SnLi is 131 °C for line radiation, 77 °C for bremsstrahlung and 70°C for neutrons heating. With an inlet temperature of 500 °C the outlet surface temperature is estimated at 707 and 780 °C for flibe and SnLi based on 1 MW/m^2 of line radiation and 0.6 MW/m^2 of Bremsstrahlung radiation. Because the evaporative flux to be discussed in the next section is a very nonlinear function of temperature, one needs to average the flux along the wall. This averaging can be parameterized by the temperature T_{eff}, with $T_{eff} > T_{ave}$.. The temperature to use in evaporation estimates, called T_{eff}, is 660 and 714 °C for flibe and SnLi.

There are three important variables, the enhanced heat transfer F or k_{eff}, largely unknown, the incident power including some of its ability to penetrate deep into the flowing liquid, and the strong variation in evaporation rate versus time all of which brings simple averaging into question.

5. Evaporation rates

Evaporation rates are estimated for use as the source term for the edge plasma calculations to estimate the contamination of the core plasma by evaporation from the liquid wall in the context of the liquid wall magnetic fusion reactors. Evaporation from a surface into a vacuum is given by

$$J = \frac{n\bar{v}}{4}, \quad \bar{v} = \sqrt{\frac{8kT}{\pi m}}, \quad n = \frac{P}{kT}, \quad J = \frac{P}{\sqrt{2\pi mkT}} \quad (7)$$

The density, n, is the density that would be present at equilibrium when evaporation equals condensation. In our case, where the edge plasma is close to the liquid surface and absorbs all evaporating particles that strike it, the density never reaches the equilibrium value but is one half of it. That is all the particles are heading away from the liquid surface. When the edge plasma is not so close or when collisions occur the equilibrium density is approached and condensation begins to cancel out evaporation. The concept of density away from equilibrium is not very useful and we will emphasize evaporation rates (number of molecules leaving the liquid per square meter per second). This is the quantity that goes into the edge plasma calculation rather than either density or vapor pressure. From experimental data in the literature the equilibrium vapor pressure is given below.

$$P(Pa) = \exp(25.63 - 24040/T) \ldots\ldots Li_2BeF_4 \ldots . BeF_2 \ \ evaporation$$

$$P(Pa) = \exp(25.92 - 22540/T) \ldots\ldots LiBeF_3 \ldots . BeF_2 \ \ evaporation \quad (8)$$

$$P(Pa) = \exp(22.35 - 22300/T) \ldots\ldots Li_{17}Pb_{83} \ldots . Pb \ evaporation$$

$$P(Pa) = \exp(22.16 - 17220/T) \ldots\ldots Li \ldots\ldots\ldots\ldots Li \ evaporation$$

$$P(Pa) = \exp(24.81 - 25800/T) \ldots\ldots Sn_{80}Li_{20} \ldots . Li \ evaporation$$

The pressure can be converted from Torr to Pa as follows: P(Pa) = 133.3×P(Torr). The dominant evaporating species is that given to the right of the pressure equation above. The BeF_2 density is 200 times LiF density. Li evaporation will be primarily Li but also some Li_2 and Li_3 will be present. The flibe vapor pressure may be inaccurate since it is extrapolated from the data at 1000 °C. The evaporation rate of the various species is plotted in Fig. 7.

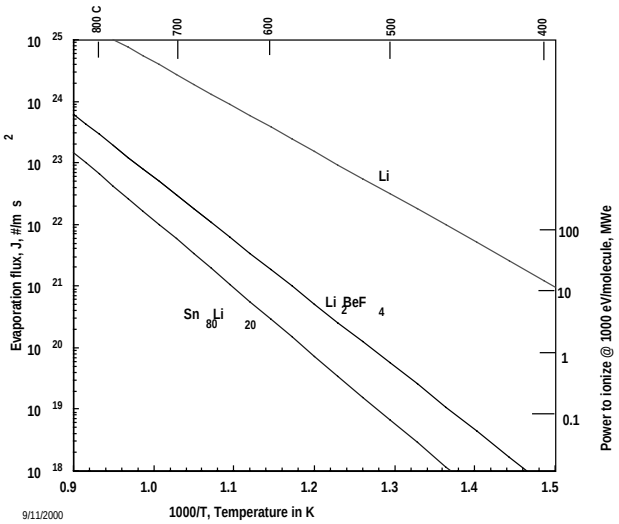

Fig. 7. Evaporation rates into vacuum for candidate liquids.

When evaporation becomes large, there are the limiting effects, which will become important for liquid wall magnetic fusion configurations and especially for liquid divertors where the evaporation is very large. These effects are: 1-collisional driven condensation of evaporated material, that is, evaporating molecules have collisions that return them to the liquid before they strike the edge plasma; 2-evaporative cooling, and 3-depletion of the volatile species at the surface. When condensation equals evaporation the latter two effects are absent. The first effect should start to become important above about 630 and 750 °C for flibe and $Sn_{80}Li_{20}$ and is expected to be especially important in the divertor. The second effect

should be important for power fluxes of 1 MW/m^2 above about 920 °C for flibe. The third effect depends on molecular diffusion rates and of course turbulence and is never expected to be important.

The distance along the FRC edge is broken into zones with zone numbers assigned as shown in Fig. 8 and calculations are made for each zone with the evaporative fluxes shown in Fig. 7 with the results shown in Fig. 9. The configuration could be oriented either horizontally as shown in Fig. 1-3 or vertically as shown in Fig. 8. For simplicity we assume the power is uniform over the cylindrical liquid wall from 4 m to -4 m at a radius of 1.5 m.

$\mathbf{A_{wall}}$ = $2\pi\times1.5\times8=75.4$ m^2
$\mathbf{V_{plasma}}$ = $4\pi\times a^2\times b/3=4\pi\times1^2\times4/3=16.8$ m^3
S = liquid flow path receiving power ≈ 8 m
L = edge plasma length = S = 8 m

The transit time of the liquid is S/V_{axial} = 8/10 = 0.8 s
Again we want to emphasize this configuration is simplified for the sake of analysis but is hopefully representative of the phenomena involved. An alternative flow path is shown in Fig. 4 with the advantages of two shorter liquid flow paths and possibly a better solution to the exit nozzle.

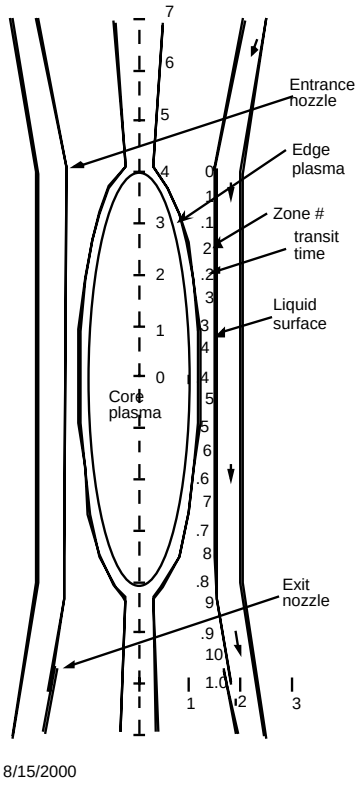

Figure 8. The FRC liquid flow model is shown. The flow path is in on one end and out on the other about 10 m in length.

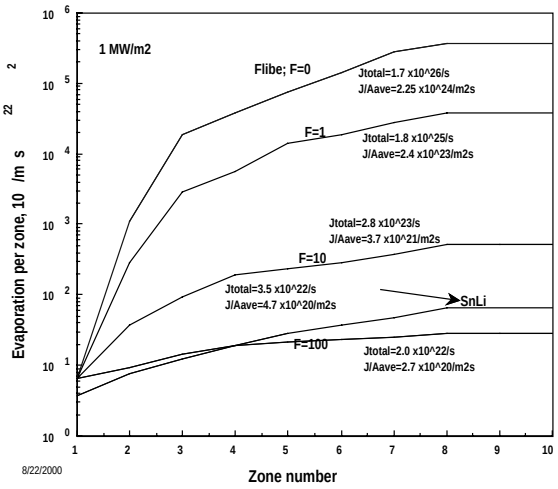

Figure 9. Evaporation per zone and total evaporation for FRC for 1 MW/m^2.

In spite of the rapid variation of evaporation rate with time and therefore distance, when the mixing is strong (F~10) or for liquid metals it makes sense to talk about an average evaporation rate corresponding to a temperature above the average temperature, called T_{eff}. For example, if the outlet temperature from Fig. 7 is 700 C and inlet is 500 C the average is 600 C, the temperature, T_{eff}, to give the average evaporation is 640 C.

6. Edge-plasma characteristics and impurity shielding

The plasma beyond the last closed magnetic flux surface is lost in an axial ion transit time out the end of the system, where it is assumed that the plasma escaping beyond the field-null region does not return from the large end-tank region. The radial thickness of the edge plasma is thus determined by a balance between the axial loss and the assumed radial diffusion from plasma turbulence. The edge plasma is especially important since it is responsible for shielding the core from the impurity vapor arising from evaporation of the liquid wall.

The plasma in the edge region is modeled by the two-dimensional plasma transport code UEDGE, which evolves equations for the plasma density, parallel ion velocity, separate electron and ion temperatures, and neutral gas density [9]. The code follows a DT fuel species, and each charge state of the impurity vapor that begins from the liquid side-wall as a neutral gas that then becomes ionized by the edge-plasma electrons.

Previously, UEDGE was used to assess the influx of impurities for a tokamak configuration [10]. For the FRC, there are two important differences: (1), the magnetic connection length along the B-field from the midplane to the effective end of the device (null-point region) is just

the physical distance of ~ 4 m for our example, much shorter than for a tokamak which has a strong toroidal magnetic field, and (2), since the divertor plate is located very far from the null-point region, recycling of neutrals can be assumed to be small. In addition, the power density from this compact device is much larger, so that more energy flux is available at the edge to ionize impurities.

For the edge-plasma calculations in the scrape-off layer (SOL) beyond the magnetic separatrix, a slab geometry is used to approximate this thin annular region. In the axial direction, the SOL plasma contacts the core boundary along an 8 m length, followed by a 2 m exit region on each end to model flow into the long dump-tank region, with negligible plasma returning from this region (i.e., low recycling). The radial domain begins at the separatrix and extends radially for 2.5 cm; the vapor gas source flows in from the outer boundary for computational efficiency, but the results are not sensitive to its location if it is placed at a larger radius. The input parameters for the core plasma edge boundary are taken from Table 1. The edge density is assumed to be 0.1 of the core density, or $2x10^{20}/m^3$. The energy flux is a total of 20 MW/m^2, split equally between ions and electrons. The anomalous radial diffusion coefficients are 0.33 m^2/s for density and 0.5 m^2/s for the ion and electron energy; these values are simply taken from tokamak experiments.

The resulting calculated DT plasma parameters in the SOL are as follows: The radial decay length for the DT fuel density is 0.38 cm. The separatrix temperatures are Te=1.44 keV and Ti=1.50 keV. The radial decay lengths for the electron and ion temperatures are 0.43 cm and 0.60 cm, respectively, although the ion temperature shows a long plateau at about 0.5 keV.

The impurity gas is injected from the side wall into the DT edge plasma, and a new multi-species plasma equilibrium in calculated. The gas flux is taken as uniform in the axial direction, and simulations with nonuniform injection to simulate the wall temperature profile shows the results are not very sensitive to this variation. The resulting impurity density at the separatrix on the midplane is shown in Fig. 10 for lithium (Li) from SnLi and for fluorine (F) from flibe as the wall gas flux is varied. For Li, there is a break in the curve at about 2 x $10^{21}/m^2$ s where there appears to be a bifurcation in the solution as Te at the wall drops below ~1 eV. Also note that fluorine penetrates to the core boundary more easily than lithium, as in the tokamak case [10], due, in part, to its higher ionization potential.

The tolerable amount of impurities in the core can be set by DT fuel dilution or radiation loss. For impurities with low to moderate maximum charge state Z, dilution is the main concern. The fractional power reduction from dilution is given by $2Z\ n_z / n_{DT}$, where n_z and n_{DT} are the impurity and DT fuel densities, respectively [10]. Thus, a 20% power reduction for lithium (Z=3) and fluorine (Z=9), sets concentration limits of 0.03 and 0.01, respectively. Since the concentration levels of relevance are deep within the core, one can make one of two assumptions about impurity density variation in the core. The first is that the impurity density is flat with the same value as at the edge, and the second is that the impurity and DT densities vary together in the core such that the concentration remains a constant. These two assumptions give two limits to the operating points in Fig. 10, labeled (for F) 1% edge and 1% core. An argument for choosing the flat density case (1% core) is that the source of impurities is on the outside, but more detailed core analysis needs to be done.

The maximum allowable edge impurity densities shown in Fig. 10 give the corresponding gas flux limits from the wall. These gas fluxes can then be plotted on curves of wall temperature versus evaporative flux as shown in Fig. 11. These points thus identify the allowable wall temperature to prevent excessive impurity intrusion into the core plasma. These initial points correspond to the base case with no intervention techniques such as auxiliary heating in the edge plasma to help ionized the impurities well away from the separatrix boundary.

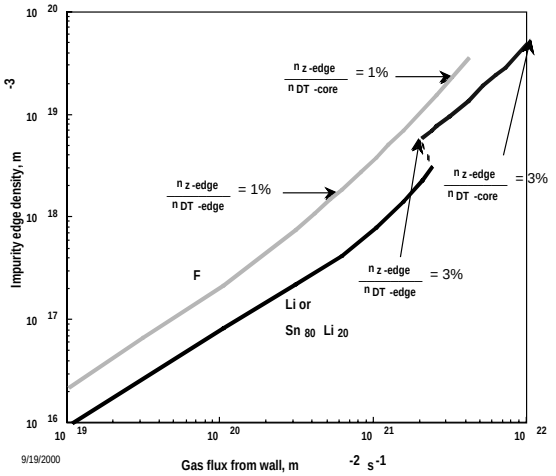

Fig. 10. Plot of impurity edge density vs average evaporation rate.

For flibe the effective temperature needs to be between 560 and 630 °C and for SnLi it needs to be between 660 and 720 °C , whereas we predicted in section 4 660 and 715 °C for flibe and SnLi.

7. Current drive by rotating magnetic fields

One option for current drive to sustain the FRC is to use rotating magnetic fields[1,11]. It was first thought to drive current by locating antennae deep (5 mean free paths or more for 14 MeV neutrons) within the low electrical conductivity molten salt. However, calculations show the

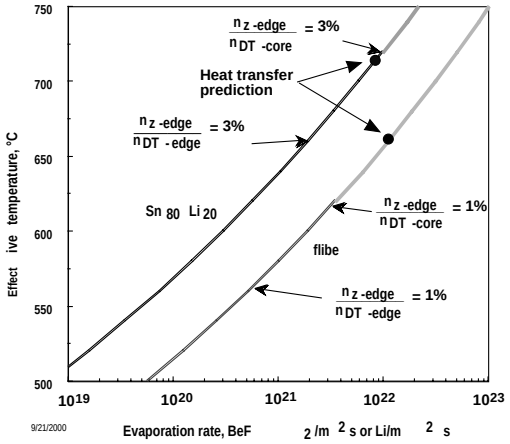

Fig. 11. Effecitve surface temperature versus evaporation rate where UEDGE says the core plasma is not overly contaminated with impurities. The dashed lines show where evaporation must be reduced by for example auxiliary edge plasma heating.

skin depth at 32 kHz to be <<0.5 m. This means that too much power would be absorbed in the near field of the antenna, leaving little to drive and sustain the current. Next we studied antenna mounted on struts or end mounted to avoid penetrations through the flowing salt. The antenna would then be located between the FRC plasma (r~ 1 m) and the flowing wall (r~1.5 m). The vapor density is ~10^{13} to 10^{14}/cm^3, which is near the minimum in the Pachen breakdown curve so discharges will easily occur. The question arises as to whether this plasma will prevent the field from penetrating outward from the antenna through the edge plasma. Apparently we do not need conductors along the field lines but rather we can rely on plasma discharge currents. Since we need to provide auxiliary power to the edge plasma to provide extra ionization and preventing or screen more of the evaporating liquid from entering the core plasma, we might as well use this discharge to drive the current that produces the rotating magnetic field for current drive. This concept of current drive will need future study to see if it is workable.
Another option for current drive is to use the compact toroid (CT) fueling method.[12]

8 Key issues and future work

1-include auxiliary edge plasma attenuation of evaporated wall material
2-study heat transfer enhancement methods to reduce the effective surface temperature
3-study rotating field current drive by the auxiliary edge plasma discharge
4-consider the geometric effect of evaporation at 1.5 m with a plasma radius at 0.39 m and include the correction for condensation

9 Conclusions

We report on moving in the direction of a self-consistent design of a thick liquid protected FRC power plant. The most important concern, that of the evaporating liquid overly contaminating the core plasma has been addressed. For flibe the evaporation seems to be too much by about an order of magnitude forcing reliance on auxiliary shielding plasmas, condensation correction to evaporation and strong enhancement of heat transfer near the free liquid surface. For SnLi the evaporation seems to be tolerable by the plasma or close to it. We are encouraged to carry out further work in this promising area of liquid wall protection for fusion power plant design.

10. Acknowledgements

*Work performed under the auspice of the U.S. Department of Energy by University of California Lawrence Livermore National Laboratory under Contract W-7405-Eng-48.

11. References

1. A. L. Hoffman, *et al.*, "The Large-s Field-Reversed Configuration Experiment," *Fusion Technology* **23,** 185 (1993).
2. H. Momota et al., "Conceptual design of the D-^{3}He reactor ARTEMIS," Fusion Technology 21 (1992) 2307-2323.
3. N. C. Christofilos, "Design for a High Power-Density Astron Reactor," J. Fusion Energy **8**, 97-105 (1989).
4. M. Abdou, APEX Interim report, UCLA-ENG-99-206 (1999).
5. The symbol for this molten salt in the past has been written as FLiBe but was made into a word with capital first letter in a fusion-spelling guide, Flibe. As usage has become more common lower case spelling has come into common use, flibe (pronunciation rhymes with tribe and scribe).
6. M. A. Hoffman and Y. T. Lee, "Performance and cost of the HYLIFE-II balance of plant," Fusion Technology **21** (1992) 1557.
7. Sergei Smolentsev, M. Abdou, N. Morley, A. Ying and T. Kunugi "K-epsilon" Model of MHD Turbulence for Free Surface Flows, submitted to "International Journal of Heat and Mass Transfer" (2000).
8. Simulation by Damir Juric, Georgia Insittute of Technology, private communications 2000.
9. T.D. Rognlien, P.N. Brown, R.B. Campbell, et al. Contr. Plasma Phys., Vol. 34 (1994) 362.
10. T.D. Rognlien and M.E. Rensink, J. Nucl. Mater., to be pub., (2000).
11. M.Ohnishi, A. Ishida, Y. Yamamoto and K. Yoshikawa, "Current Sustainment of a Field-Reversed

Configuration by Rotating Magnetic Field," Trans. Fusion Technol. 27, 391 (1995).
12. Perkins, L.J., S.K. Ho, and J.H. Hammer, "Deep Penetration Fueling of Reactor-Grade Tokamak Plasmas with Accelerated Compact Toroids," *Nuclear Fusion* **28,** 1365 (1988).